Subcutaneous Adipose Tissue Response to a Non-Invasive Hyperthermic Treatment Using a 1,060 nm Laser

John W. Decorato, MD, FACS,[1]* Bo Chen, PhD,[2] and Rafael Sierra, PhD[2]
[1]*Private Practice in Plastic Surgery, Staten Island, New York*
[2]*Cynosure, Inc., Westford, Massachusetts*

Background: We postulated that a hyperthermic treatment using a 1,060 nm laser can cause a controlled adipocyte injury resulting in non-invasive fat reduction. This three-part study identified treatment parameters for a safe and tolerable treatment, demonstrated short- and long-term tissue response, and assessed the potential of this treatment for non-invasive fat reduction.
Methods: In vivo temperature measurements were conducted prior to abdominoplasty *via* a thermal camera (for surface readings) and thermocouple needle (for subcutaneous readings). Short- and long-term tissue response was evaluated on the abdomen immediately post to 6 months post a 1,060 nm laser treatment. Laser dosage was varied to identify safe and effective parameters for fat reduction. Tissue biopsies for hematoxylin/eosin (H&E) staining were taken at weeks 1 and 2, as well as at 1, 2, 3, and 6 months (if applicable). Additionally, six subjects received a hyperthermic laser treatment to the flanks; four patients receiving laser treatment to one flank and cryolipolysis on the other, and two patients receiving laser treatment on one side with the other side as an untreated control. Efficacy measurements included ultrasound measurement of fat thickness at baseline, 2, 3, and 6 months; Magnetic Resonance Imaging (MRI) to calculate fat volume at baseline, 3 and 6 months; and blinded photograph evaluation at baseline, 1, 2, 3, and 6 months.
Results: In vivo temperature measurements demonstrated that the hyperthermic temperature target (42–47°C) can be achieved and maintained in subcutaneous adipose tissue *via* a 1,060 nm laser in conjunction with surface cooling. Short- and long-term tissue responses were evaluated by tissue histology up to 6 months following treatment. Histological changes included inflammation, followed by macrophage infiltration starting at approximately 2 weeks, with evacuation of cellular debris completed by approximately 6 months. Clinical results demonstrated average fat thickness reduction at 14%, 18%, and 18% at 2, 3, and 6 months, respectively. Average fat volume reduction measured by MRI at 3 and 6 months was 24% and 21%, respectively. Blinded photo evaluation showed improvement starting at 1-month post-treatment and was maintained at 6 months. Adverse events were rare and included mild tenderness that resolved by 1-week post-treatment.
Conclusion: Parameters were identified that selectively injure and reduce adipocytes in subcutaneous tissue using a 1,060 nm externally applied laser. The treatment had an excellent safety profile and was well tolerated. The clinical study demonstrated that a 1,060 nm hyperthermic laser treatment for non-invasive fat reduction can be safe and effective. Lasers Surg. Med. © 2016 Wiley Periodicals, Inc.

Key words: body contouring; non-invasive body contouring; non-invasive fat reduction; laser fat reduction

BACKGROUND

Liposuction has been the most common modality [1] for fat reduction and body contouring, but associated risk included post-operative morbidity, recovery, and downtime [2]. Alternative or adjunctive methods for localized fat destruction such as lasers [3], high-intensity focused ultrasound [4,5], radiofrequency devices [6], and selective cryolipolysis [7,8,9,10,11] are increasingly being utilized to reduce downtime. We explored the use of increased temperature delivered *via* externally applied laser to reduce fat.

Thermal injury to biological tissue has been widely studied. The basic biophysical chemistry equation, known as the Arrhenius equation, can be used to calculate the relationship of tissue damage to exposure time and tissue temperature [12]. A damage parameter Ω is used to indicate the level of damage (Appendix A). Many studies suggested that a moderate temperature rise (5–10°C) with prolonged exposure time (minutes to hours) will cause cellular and tissue injury. Studies on the effects of heat on various cell types have included *in vitro* and animal experiments in which a direct cell-killing effect at temperatures ranging from 42 to 47°C was demonstrated. Hyperthermic cell death has been shown to be markedly enhanced at temperatures exceeding 43°C and/or in

Conflicts of Interest Disclosures: All authors have completed and submitted the ICMJE Form for Disclosure of Potential Conflicts of Interest and none were reported.
*Correspondence to: John W. Decorato, MD, FACS, Private Practice in Plastic Surgery, Staten Island, New York.
E-mail: jwd@drdecorato.com
Accepted 5 December 2016
Published online in Wiley Online Library (wileyonlinelibrary.com).
DOI 10.1002/lsm.22625

© 2017 Wiley Periodicals, Inc.

combination with radiation and various cytostatic drugs by sensitization [13,14]. The effect of mild hyperthermia on adipocytes has been demonstrated by several earlier studies as well. One investigation of cell membrane physiology demonstrated that raising temperatures 6°C above normal (i.e., 43°C), resulted in the loss of the structural integrity of the lipid bilayer [15]. A study on cell membrane permeability [16] indicated that the cell membranes showed evidence of damage when heated to 45°C for more than 5 minutes. A third study of *in vitro* cell culture and *in vivo* human adipose tissue demonstrated that 15 minutes of thermal exposures to 43–45°C resulted in delayed adipocyte death [6]. As with cryolipolysis, which decreases subcutaneous tissue temperature below body temperature and maintains it for prolonged period of time (60 minutes), a hyperthermic laser treatment which raises adipose tissue temperature to 42–47°C for a sustained time is proposed to cause adipocyte injury with a similar therapeutic reduction outcome.

The purpose of this three-part investigation was to test the hypothesis that exposure of subcutaneous adipose tissue to hyperthermic temperature over a period of time using an external 1,060 nm laser device can: (i) safely induce therapeutic adipocyte injury; (ii) damage adipocytes that will subsequently be cleared by inflammatory processes; and (iii) cause volume of adipose tissue to decrease.

MATERIALS AND METHODS

Laser System

A prototype diode laser system was developed utilizing four 1,060 nm diode bars directly coupled into a treatment handpiece. This handpiece was fitted with a water-cooled sapphire window $3 \times 10 cm^2$ at the point of skin contact. An optical diffuser and reflectors were deployed to create a uniform 1,060 nm radiation field. Output could be adjusted with irradiance up to $5 W/cm^2$ and pulse durations from 100 ms to continuous. The absorption curves of skin and fat at $1,060 \pm 20$ nm are rather flat. Therefore, diode laser was chosen over a Nd:YAG laser due to ease of control and lower cost.

Study Design

The study consisted of three parts. Subject demographics for all three parts of the study are summarized in Table 1.

Part 1: In vivo temperature measurement. In vivo temperature was recorded to validate laser parameters and verify estimates from a laser heating model. Tests were conducted on the abdomen of four subjects under general anesthesia prior to abdominoplasty. Temperature measurements were performed using a thermal camera (FLIR ThermaCAM® E45, Niceville, FL) and a thermocouple needle (Ellab, Centennial, CO) to map the temperature distribution from the skin's surface to a depth of 3 cm with titrated treatment parameters. Surface temperature was recorded before and immediately following laser exposure using a thermal camera. The thermocouple needle has a temperature accuracy of 0.1°C and a response time of 0.3 seconds. A sterile thermocouple needle was introduced at depths of 0.5, 1.0, 1.5, 2.0, 2.5, and 3.0 cm and treatment was paused during measurement to avoid direct heating of the thermocouple. Immediately after treatment, tissue biopsies were obtained to evaluate acute tissue response.

TABLE 1. Study Design

Study part	No. of subjects	Type of subjects	Treatment area
#1	4	Subjects were tested under general anesthesia right before the abdominoplasty	Abdomen
#2	12	Subjects were treated with laser 1–6 months before abdominoplasty	Abdomen
#3	6	Subjects were treated with non-invasive fat reduction treatment only	Flank

Part 2: Short- and long-term tissue response to treatment. Using the findings in part 1, system parameters capable of generating subcutaneous adipose tissue hyperthermia were determined. Twelve subjects scheduled for abdominoplasty were recruited for this part of the study. Total exposure time and laser duty cycles (Table 2) were varied to identify a safe and effective dosage range based on evaluation of tissue histology and side effects. Up to five areas on the abdomen of each subject were used for testing. Subjects were treated 1–6 months prior to their abdominoplasty. All subjects were awake during treatment and pain management was not required. Blood samples were obtained for monitoring lipid and liver chemistry and tested at specific points along the study timeline (baseline, 3, 7, 14, and 30 days; and 2, 3, and 6 months post-laser treatment). Side effects were recorded. Tissue biopsies with hematoxylin/eosin (H&E) staining were obtained at multiple follow-up intervals from 1 and 2 weeks to 1, 2, 3, and 6 months after treatment. Biopsies at 1 and 2 weeks were obtained through a core biopsy needle during patient follow up. Biopsies at 1–6 months were obtained from excised tissue post abdominoplasty. Four evenly spaced surgical biopsies within the treatment area were obtained. The biopsy specimens were roughly 10 mm by 5 mm in size and included skin and approximately 2 cm of subcutaneous tissue.

Part 3: Pilot clinical study on flanks. Based on the results of the second part, a set of treatment parameters were identified. The third part included a pilot study of non-invasive fat reduction on the flanks. Six subjects were recruited for flank treatment and divided into two groups (healthy Caucasian women, average BMI of 25, BMI range 21.8–28.4). Subjects were excluded if the subject had hereditary factors which can affect the body's ability to store fat, or had previous liposuction/liposculpture or any type of procedure in the treatment area.

TABLE 2. Tissue Response to Various Laser Dosages

	Duty cycle		
Tx time	60–65%	66–70%	71–78%
8 minutes			Fat damage: 0/3[a] subjects Nodule: 0/3 subjects
15 minutes		Fat damage: 2/2 subjects (Focal fat damage < 5 mm) Nodule: 0/2 subjects	
20 minutes	Fat damage: 0/1 subject Nodule: 0/1 subject	Fat damage: 3/3 subjects Nodule: 0/3 subjects	Fat damage: 2/2 subjects Nodule: 0/2 subjects
25 minutes	Fat damage: 1/2 subjects (focal fat damage <5 mm) Nodule: 0/2 subjects	Fat damage: 7/7 subjects Nodule: 0/7 subjects	Fat damage: 2/2 subjects Nodule: 0/2 subjects
30 minutes		Fat damage: 1/1 subject Nodule: 0/1 subject	Fat damage: 3/3 subjects Nodule: 2/3 subjects
45 minutes		Fat damage: 2/2 subjects Nodule: 1/2 subjects	Fat damage: 3/3 subjects Nodule: 3/3 subjects

[a]0/3 means 0 out of 3 tested subjects showed sign of fat damage from histology analysis.

Subjects were instructed to maintain their current weight and not change their diet or exercise routine. In group one, two patients underwent laser treatments on one flank with the contralateral side left untreated as a control. In group two, four patients underwent laser treatment on one flank and cryolipolysis on the contralateral flank. Laser treatment was performed using a prototype 1,060 nm diode laser device, with an exposure time of 25 minutes. The size of the laser radiation window was 90 cm^2. The actual treatment area in the subcutaneous layer (although not measured for this prototype system) should be larger based on another study conducted by Doherty et al. [17]. The study by Doherty et al. demonstrated a larger thermal footprint in subcutaneous layer as compared to the size of the laser radiation window due to light scattering and heat diffusion. Cryolipolysis was performed using the CoolSculpting® system (ZELTIQ® Aesthetics, Inc., Pleasanton, CA) with the standard Zeltiq eZ App 6.3 handpiece (CoolCore™), treatment time was 60 minutes.

Efficacy was evaluated *via* ultrasound (US) imaging, MRI, and blinded photo evaluation. Fat thickness was measured by ultrasound using Sonosite Micromaxx (Sonosite, Bothell, WA) system (transducer HFL38/13-6 MHz) at baseline as well as 2, 3, and 6 months after treatment. The same technician performed each ultrasound exam using a validated technique to ensure consistency. A transducer holder was used to standardize the pressure applied on the skin and avoid spurious thickness measurements. Ultrasound images were taken during a relaxed exhalation breath-holding period, and at nine evenly spaced locations on each flank. The US locations were recorded at baseline for consistency using a height scale with laser beam to record the vertical medial and lateral edge and a tape ruler to record the horizontal edges to the umbilicus.

MRI images were used to evaluate the entire flank and to calculate fat volume at baseline as well as 3 and 6 months post-treatment. Fat volume measurements were calculated using images taken in the transverse planes. Subjects were positioned supine in the magnet with their arms above their heads; images were captured during a relaxed exhalation breath-holding period; nine evenly spaced transverse images of each treated flank were used to calculate fat volume. Transverse imaging was performed from 10 cm above the treatment level to10 cm below the treatment level. Slice thickness was 5.5 mm.

Photographic evaluation by blinded expert evaluators (board-certified plastic surgeons) comparing baseline to post-treatment was based on standardized 2D photographs taken by a professional photographer in a controlled setting at baseline as well as 1, 2, 3, and 6 months. Body contouring outcomes were graded based on a 0–4 scale (0 = worse, 1 = no change, 2 = slight improvement, 3 = moderate improvement, and 4 = significant improvement).

RESULTS

In Vivo Temperature Measurement

Figure 1A and B graphically demonstrate the temperature distribution in tissue measured in two subjects. The skin cooling window temperature was set at 15°C. Figure 1A shows the temperature at the center of the treatment area at various depths before and after 8 minutes of laser exposure. Skin surface temperature remained below 30°C during the entire exposure. Peak temperature in adipose tissue was located at 1–1.5 cm deep with a relatively flat temperature gradient. In this case, target temperature (42–47°C) was achieved and maintained from 1 to 3 cm. Figure 1B illustrates the tissue temperature at various time points during laser irradiation. Based on these measurements, a set of system parameters was developed

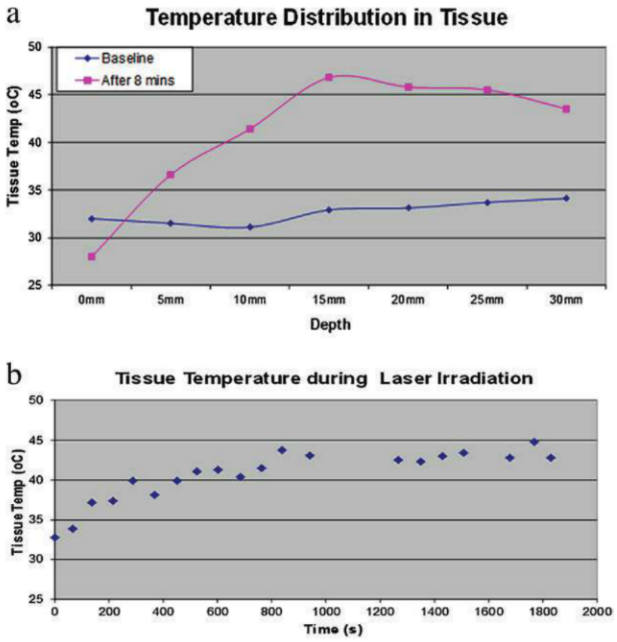

Fig. 1. (**a**) Temperature distribution in tissue. Temperature at center of treatment area after 8 minutes laser Tx. Tissue temperature at 0 mm was measured by a thermal camera. Tissue temperature at various depths was measured by a thermocouple. (**b**) Temporal temperature distribution during a laser treatment. Tissue temperature was measured by a thermocouple at the center of treatment area.

which would promote hyperthermia in subcutaneous adipose tissue without elevating skin temperature >30°C during laser exposure (surface cooling temperature 15°C, laser irradiance 1–2 W/cm^2 with laser duty cycle 60–80%). Skin surface temperature was maintained below 30°C for skin safety as well as patient comfort [18]. Laser exposure was modulated to maximize patient comfort. Duty cycle was calculated based upon the laser on and off time during every 30 seconds cycle.

Laser Dosage

Up to five test areas on each of the 12 subjects abdomens were treated with different treatment times and laser duty cycle settings (Table 2). Tissue response to various treatment settings was studied to determine safe and effective parameters. Measurement of size of the affected area and histological evaluation of adipocyte damage was used to gauge efficacy. As seen in Table 2, treatment longer than 30 minutes caused the development of palpable nodules in deep fat consistent with clinical findings of fat necrosis. These nodules were observed at 1 month post-treatment and did not resolve at 6 months. The 6-month nodule (Fig. 2), resulting from higher dosage exposure (treatment time 45 minutes), demonstrated extreme pathological changes with "ghost-like" mummified fat cells at the center, surrounded by fibrosis and cystic spaces consistent with encapsulated fat necrosis. For treatment time less than 20 minutes, histological analysis and gross measurement of treatment zone demonstrated either a small area of effect (<0.5 cm) or no discernible damage to adipose tissue. Data analysis suggested optimal treatment time of 20–25 minutes and duty cycle equal or higher than 66%. No long-term nodule development was noted at these settings. Long-term histology showed the injury site can be cleared through the body's inflammatory processes (discussed in the next paragraph).

Vital signs during and after treatment were monitored and no significant differences before, during, or after treatment were noted. Blood testing of lipid and liver chemistry was conducted at baseline and throughout the 6-month study period (days: 3, 7, 14, 30, and months: 2, 3, 6), and included total cholesterol, high density lipoprotein (HDL), triglycerides, low density lipoprotein (LDL), non-LDL cholesterol, glucose, alanine aminotransaminase (ALT), aspartate aminotransaminase (AST), total protein, alkaline phosphatase, total bilirubin, and albumin. No significant changes were seen at any time in any of the measured assays.

Short- and Long-Term Tissue Response

Histology immediately after laser treatment showed no apparent evidence of adipocyte injury on H&E stain. At 5–7 days there was evidence of inflammatory change. By day 14, adipocytes demonstrated changes consistent with early damage. One month after the treatment, adipocyte damage was identified in the lobules and there were numerous macrophages surrounding the remaining adipocytes. By 2–3 months, foamy macrophages surrounded adipocytes and cystic spaces of variable size were identified; clear areas of increased fibrosis were identified as well. By 6 months, there was greater fibrosis and fewer foamy macrophages present compared to the 3-month time point. Results of the histology are shown in Figure 3. Skin showed no sign of damage at any time point as anticipated, with skin temperature below 30°C during treatment.

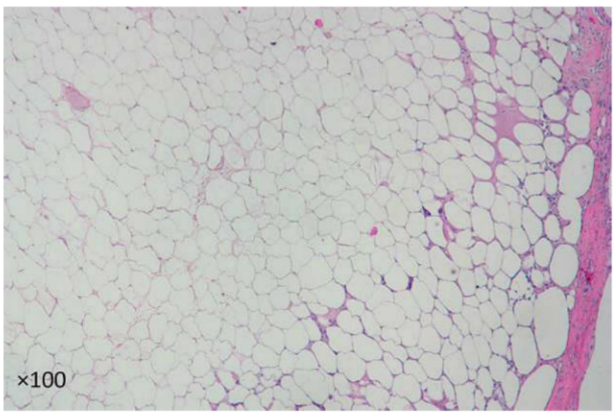

Fig. 2. Histology of nodule at 6 months. The site treated with higher dosage (45 minutes treatment time) has "ghost-like" mummified fat cells at the center, surrounded by fibrosis and cystic spaces as can be seen in the clinical entity known as encapsulated fat necrosis.

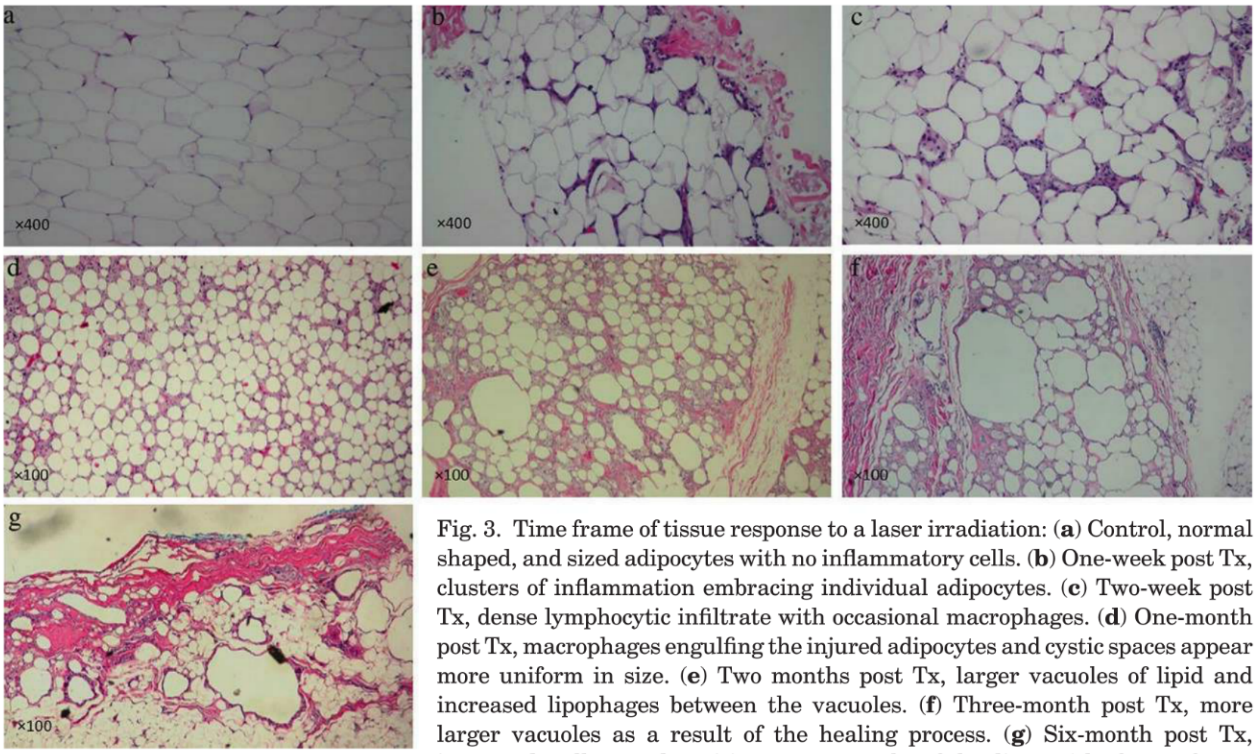

Fig. 3. Time frame of tissue response to a laser irradiation: (**a**) Control, normal shaped, and sized adipocytes with no inflammatory cells. (**b**) One-week post Tx, clusters of inflammation embracing individual adipocytes. (**c**) Two-week post Tx, dense lymphocytic infiltrate with occasional macrophages. (**d**) One-month post Tx, macrophages engulfing the injured adipocytes and cystic spaces appear more uniform in size. (**e**) Two months post Tx, larger vacuoles of lipid and increased lipophages between the vacuoles. (**f**) Three-month post Tx, more larger vacuoles as a result of the healing process. (**g**) Six-month post Tx, increased collagen deposition as a result of healing with fewer foamy macrophages when compares to 3 months post Tx.

Clinical Evaluation of Flank Treatment

Tables 3 and 4 summarize the changes in fat thickness and volume. The untreated control side showed minimal changes in ultrasound and MRI measurements at 2, 3, and 6 months (Table 3). In group 2, laser treatment average fat thickness as measured by ultrasound (samples of US imaging were shown in Fig. 4), was reduced at 3-time points (14%, 18%, and 18% at 2, 3, and 6 months, respectively), compared to the cryolipolysis side showing average reductions of 14%, 17%, and 16%, respectively. Average fat volume reductions 3 and 6 months after laser treatment, measured by MRI as shown in Figure 5, were 24% and 21%, respectively, with the cryolipolysis treatment side showing 22% and 19% reductions. Blinded photo grading demonstrated cosmetic improvement at 1 month (improvement score 2.3), and was maintained over 6 months (Fig. 6B). Figure 6A highlights treatment effects *via* overlay of before and after pictures.

Adverse events on the laser side were mostly mild tenderness that resolved within 1 week. Adverse events on the cryolipolysis side were bruising and mild to moderate numbness which resolved within 1–4 weeks. No long-term side effects were recorded for either treatment.

DISCUSSION

This study demonstrated that prolonged exposure of subcutaneous adipose tissue to hyperthermic temperatures can cause clinically relevant adipocyte injury non-invasively. Evaluation of laser dosage identified the ideal treatment time as between 20 and 25 minutes. At >30 minutes, there was a risk of developing persistent palpable subcutaneous nodules, while treatment times of <20 minutes were associated with a sub-optimal effect. Inflammation was noted histologically and injured adipocytes were gradually removed by inflammatory processes over several months. There was no damage to the skin and no statistically significant changes in blood lipid or liver chemistry. Ultrasound, MRI, and photographic evaluations showed noticeable fat reduction starting at 1 month and maintaining through the 6-month follow up. In group 1, the untreated side showed minimal changes at all follow up intervals. This supported our hypothesis that the fat reduction measured on the laser side was a result of the treatment. In group 2, the cryolipolysis side showed average 17% fat thickness and 22% volume reduction at 3 months. These results were similar to reports from other group's study on flanks treated by cryolipolysis [8]. It further validated our evaluation methods, and showed that our objective evaluation of fat reduction (US and MRI) can obtain consistent results as compared to other modalities.

The 1,060 nm wavelength was selected due to its optical properties in skin and fat. When compared to other visible or infrared wavelengths, 1,060 nm is known to have minimal absorption in the skin making it a more efficient wavelength for delivering laser energy through the skin to the subcutaneous target. Its low affinity for melanin makes safe treatment of darker skin feasible, although this was not studied in this paper. Relatively higher penetration

TABLE 3. Fat Thickness and Volume Reduction, Group 1: Laser Versus Untreated

			Fat thickness (ultrasound) [mm (%)][a]			Fat volume (MRI) (cc [%][a])	
			Time post-treatment				
Pt. no.	Weight change at 6-month	Treatment	2 months	3 months	6 months	3 months	6 months
5	+12 lbs	Laser	2.4 (14%)	2.6 (15%)	1.1 (6%)	16.7 (16%)	9.2 (9%)
		Untreated	0.6 (3%)	0.9 (4%)	−1.4 (−6%)	8.7 (8%)	−1.4 (−1%)
6	−2 bs	Laser	4.0 (14%)	3.3 (12%)	3.6 (13%)	15.9 (10%)	17.0 (11%)
		Untreated	−0.3 (−2%)	−0.8 (−4%)	−0.4 (−2%)	−8.3 (−5%)	0.0 (0%)
Average and standard deviation		Laser	3.2 ± 1.1 (14 ± 0%)	3.0 ± 0.5 (14 ± 2%)	2.4 ± 1.8 (10 ± 5%)	16.3 ± 0.6 (13 ± 4%)	13.1 ± 5.5 (10 ± 1%)
		Untreated	0.2 ± 0.6 (1 ± 4%)	0.1 ± 1.2 (−1 ± 6%)	−0.9 ± 0.7 (−4 ± 3%)	0.2 ± 12.0 (2 ± 9%)	−0.7 ± 1.0 (−1 ± 1%)

[a]Change from baseline.

TABLE 4. Fat Thickness and Volume Reduction, Group 2: Laser Versus Cryolipolysis

			Fat thickness (ultrasound) [mm (%)][a]			Fat volume (MRI) (cc [%])	
			Time post-treatment				
Pt. no.	Weight change at 6 months	Treatment	2 months	3 months	6 months	3 months	6 months
1	−4 lbs	Laser	10.4 (26%)	12.1 (30%)	14.0 (35%)	54.7 (37%)	49.0 (33%
		Cryolipolysis	2.0 (8%)	1.9 (8%)	3.8 (15%)	54.7 (30%)	36.7 (20%)
2	−3 lbs	Laser	3.9(15%)	3.0 (11%)	3.2(12%)	33.8 (19%)	35.0 (20%)
		Cryolipolysis	0.6 (4%)	1.2 (7%)	1.2 (7%)	5.4 (3%)	12.6 (7%)
3	−3 lbs	Laser	−1.0 (−6%)	1.6 (10%)	1.2 (7%)	32.4 (20%)	14.8 (9%)
		Cryolipolysis	3.9 (20%)	5.2 (27%)	3.4 (17%)	38.6 (25%)	34.0 (22%)
4	0 lbs	Laser	3.0 (20%)	2.7 (19%)	2.5 (17%)	20.8(21%)	20.0 (20%)
		Cryolipolysis	4.9 (24%)	5.3 (27%)	4.6 (23%)	39.7 (29%)	37.3 (27%)
Average and standard deviation		Laser	4.1 ± 4.7 (14±14%)	4.9 ± 4.9 (18±9%)	5.2 ± 5.9 (18±12%)	35.4 ± 14.1 (24±9%)	29.7 ± 15.5 (21±10%)
		Cryolipolysis	2.9 ± 1.9 (14±10%)	3.4 ± 2.2 (17±11%)	3.3 ± 1.5 (16±7%)	34.6 ± 20.8 (22±13%)	30.2 ± 11.8 (19±9%)

[a]Change from baseline.

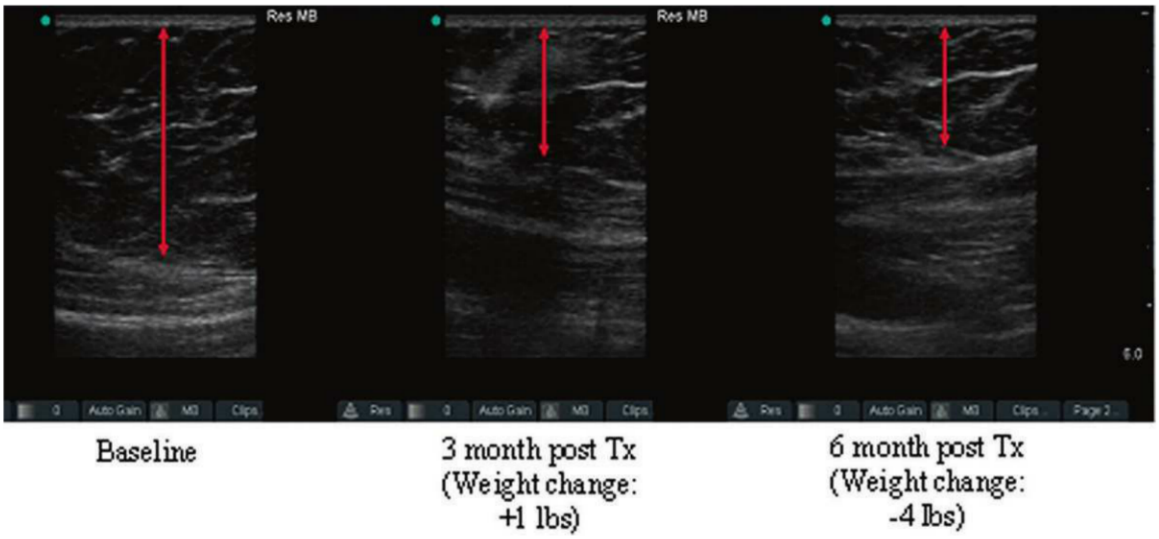

Fig. 4. Ultrasound images of adipose layer before and post Tx. Ultrasound images were taken from the same patient at the same site over a 6-month period. The arrow demonstrated the thickness of the adipose layer.

depth in fat compared to other wavelengths in the visible to infrared spectrum facilitates spreading of heat over a larger volume without creating a sharp temperature gradient, or hot spot. The maximum tolerable temperature in tissue is limited by perceived patient discomfort where the maximum temperature is reached. The treatment design is to create a flat temperature gradient along the direction of laser propagation, so large volumes of subcutaneous tissue can be heated to therapeutic temperature before maximum tolerable temperature is reached. Previous attempts using the lipid favorable 1,210 nm wavelength were tested by Anderson et al. [19] to non-invasively destroy subcutaneous tissue through coagulation within a few to tens of seconds. However, the lipid favorable 1,210 nm wavelength is not a preferable choice in our treatment design. Compared to the 1,060 nm wavelength, the 1,210 nm is less efficient in delivering laser energy through skin due to its higher absorption. Additionally, the 1,210 nm wavelength has less penetration depth in fat, which will create a sharper temperature gradient during exposure and therefore create a less effective treatment zone. The choice of wavelength, along with the use of a specifically designed slow laser heating algorithm (explained in next paragraph), significantly increased the overall effective treatment zone (volume of tissue reaching hyperthermic temperature during

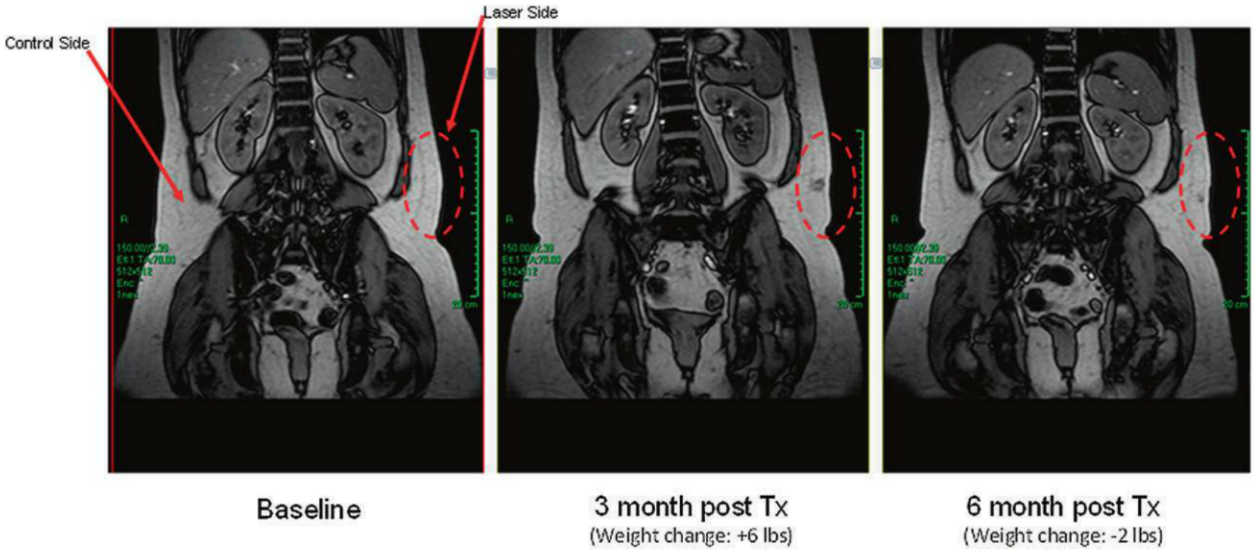

Fig. 5. Examples of fat thickness changes demonstrated by MRI.

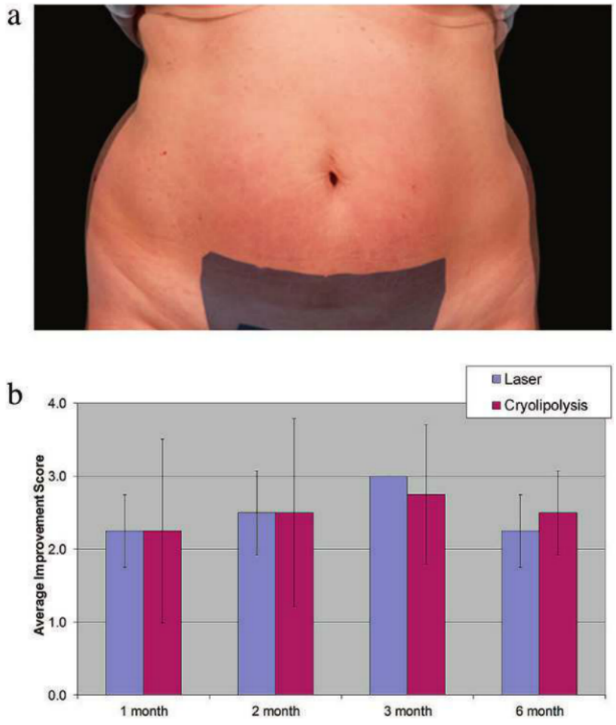

Fig. 6. (**a**) Overlay picture of one subject before and after treatment. Patient right flank treated by Cryolipolysis and left flank treated by a 1,060 nm laser. Weight change: +1 lbs. (**b**) Average improvement score of four subjects in group 2.

treatment) in subcutaneous tissue as demonstrated by *in vivo* temperature measurements (Fig. 1A). The temperature gradient along the laser propagation vector was rather flat. Figure 1A showed at least 2 cm thickness of adipose tissue was heated to the therapeutically relevant target temperature range at depths between 1 and 3 cm.

Due to thermal conduction, the extent of the thermal effect in tissue from this treatment design is much deeper than optical penetration depth alone. Therefore, the thermal response to the laser radiation is governed by conduction. This is a time- as well as a spatial-dependent process that establishes a spatial temperature gradient. Establishing a desirable temperature gradient is one of the goals of the current design. Thermal relaxation time is the time required for the temperature of a tissue structure to decay by a given amount, commonly 50%, as a result of conduction. The thermal relaxation time is a convenient parameter that can be used to characterize the length of time heat is primarily confined to the target tissue. Because the size of the laser applicator is much larger than the penetration depth of 1,060 nm wavelength radiation, the time constant in the present application can be estimated based on a one-dimensional axial time constant, approximated by: $\tau_z \approx a/(\alpha\mu_{eff}^2)$. Here, a is a constant that depends only on the geometry of the target and is usually of the order of magnitude of 1. The parameter $\alpha = k/(\rho C)$, where k is the thermal conductivity of the tissue, ρ the density, and C the heat capacity. Finally the parameter μ_{eff} is the effective attenuation coefficient at 1,060 nm including both absorption and scattering. Even using a generous estimate, the thermal relaxation time is on the order of a few 100 seconds which is much shorter than the treatment time (25 minutes). The dynamic balance of heating and cooling determines the temperature distribution. The settings of cooling, laser power, and exposure time are established and creates the desired temperature distribution as demonstrated in Figure 1A. This distribution insures that the skin and a few millimeters of the superficial layer of subcutaneous fat are kept at a temperature below what is needed to cause damage throughout the treatment.

The thermal properties of lipid-rich adipose tissue as compared to water rich tissue are in favor of safety. The temperature rise, in the absence of heat loss from conduction and blood perfusion, was proportional to density (ρ) and heat capacity (C). $E=\rho CV\Delta T$, where E is energy absorbed in a volume (V). ΔT is the temperature change. Water-rich tissue has a higher density and heat capacity than lipid rich tissue. For example, the ρC value for muscle is approximately 2.5 times higher than that of subcutaneous adipose tissue; therefore, for the same amount energy absorbed, average temperature rise in muscle would be 2.5 times less than in adipose tissue.

The present study, as well as other published studies on tissue damage [18,20–22], suggest that adipocytes are more susceptible to temperature alteration (cold or heat) as compared to other neighboring cells. Study of cryolipolysis, the application of controlled cooling to non-invasively damage subcutaneous adipocytes, has shown increased susceptibility of lipid-rich adipocytes to cold injury as compared to surrounding water-rich cells. A preclinical porcine study demonstrated that damage to subcutaneous fat without damage to the overlying skin and underlying muscle was possible [7]. Evidence from studies on thermally damaged cells has also shown that increased susceptibility of adipocytes to heat may also be true. Our study shows that adipocyte damage can be created with a treatment involving 25 minutes heating at a temperature in the range 42–47°C. Consistent with the temperature distribution described above and the difference in susceptibility to thermal damage to the various tissues, histology from our study shows no sign of damage in the epidermis, dermis, and fibrous septae in the subcutaneous tissue. Absence of bruising, hematomas, or seromas suggest that large blood vessels remained undamaged. We do not expect any damage to the nerve, fascia, and muscle-based on thermal and optical analysis. The side effect profile from long term subjects can support this claim to some extent but may be insufficient. We did not conduct any specific exam or histology on nerve or muscles in the study since the damage to these tissues were not expected. Skin is cooled during treatment which inhibited comparison of thermal susceptibility between adipocytes and skin cells. Even if the skin is exposed to the same level of heat generated within adipose tissue, we do not expect skin damage as suggested by calculated damage parameter Ω (Appendix A). Appendix A provides a comparison of various tissue damage predicted by a thermal damage model. The

TABLE 5. Published Tissue Damage Rate Process Coefficients [1,7,8,15,22]

Damage endpoint	Model	E_0 [J/mole]	A [1/s]	Ω^*
Trans-epidermal necrosis, (pig skin)	Henriques	6.27×10^5	3.1×10^{98}	0.25
Birefringence loss in skin collagen, (rat skin)	Pearce	3.06×10^5	1.606×10^{45}	0.03
Protein and enzyme denaturation	Birngruber	2.93×10^5	10^{44}	0.24
Aorta (collagen)	Agah	4.3×10^5	5.6×10^{63}	0.0006

*Ω was calculated based on a constant 47°C temperature and 25 minutes time.

results of the model support the assertion that adipocytes are more susceptible to heat.

The small size of the investigation is its key limitation. Further study using larger populations would be advantageous to confirm and strengthen conclusions drawn from safety and efficacy data as well as validate comparison outcomes and provide stronger control data. Inclusion of patients with darker skin types would also confirm safety when treating those populations.

CONCLUSIONS

Tissue temperature measurements as well as clinical and histological evaluations of *in vivo* tissue identified parameters that can be used to damage subcutaneous adipose tissue effectively using a 1,060 nm laser applied to the skin. This method has an excellent safety profile and was well tolerated. Histologic, quantitative measurements, and blinded evaluation of aesthetic improvement demonstrated that the 1,060 nm hyperthermic treatment results in safe non-invasive fat reduction.

ACKNOWLEDGMENTS

The authors thank Anne Allan, MD for analyzing the histological samples and Mirko Mirkov, PhD for his assistance in constructing the prototype laser device.

REFERENCES

1. American Society for Aesthetic Plastic Surgery. Statistics. Cosmetic Surgery National Data Bank. 2013. Accessed January 28, 2015.
2. Kim YH, Cha SM, Naidu S, Hwang W. Analysis of postoperative complications for superficial liposuction: A review of 2398 CasesPlast. Reconstr Surg 2011;127:863–871.
3. Lach E. Reduction of subcutaneous fat and improvement in cellulite appearance by dual-wavelength, low-level laser energy combined with vacuum and massage. J Cosmet Laser Ther 2008;10(4):202–209.
4. Ascher B. Safety and efficacy of UltraShape Contour I treatments to improve the appearance of body contours: Multiple treatments in shorter intervals. Aesthet Surg J 2010;30(2):217–224.
5. Pearce JA, Thomsen S. Kinetics for birefringence changes in thermally coagulated rat skin collagen. Proc SPIE 1993;1876: 180–185.
6. Franco W, Kothare A, Ronan SJ, Grekin RC, McCalmont TH. Hyperthermic injury to adipocyte cells by selective heating of subcutaneous fat with a novel radiofrequency device: Feasibility studies. Lasers Surg Med 2010;42(5):361–370.
7. Manstein D, Laubach H, Watanabe K, Farinelli W, Zurakowske D, Anderson RR. Selective cryolysis: A novel method of non-invasive fat removal. Lasers Surg Med 2008;40:595–604.
8. Avram MM, Harry RS. Cryolipolysis for subcutaneous fat layer reduction. Lasers Surg Med 2009;41(10):703–708.
9. Klein KB, Zelickson B, Riopelle JG, Okamoto E, Bachelor EP, Harry RS, Preciado JA. Non-invasive cryolipolysis for subcutaneous fat reduction does not affect serum lipid levels or liver function tests. Lasers Surg Med 2009;41(10):785–790.
10. Zelickson B, Egbert BM, Preciado J, Allison J, Springer K, Rhoades RW, Manstein D. Cryolipolysis for noninvasive fat cell destruction: Initial results from a pig model. Dermatol Surg 2009;35:1–9.
11. Krueger N, Mai SV, Luebberding S, Sadick NS. Cryolipolysis for noninvasive body contouring: Clinical efficacy and subject satisfaction. Clin Cosmet Investig Dermatol 2014;7:201–205.
12. He X, Bischof JC. Quantification of temperature and injury response in thermal therapy and cryosurgery. Crit Rev Biomed Eng 2003;31(5-6):355–422.
13. Dewey WC. Arrhenius relationships from the molecule and cell to the clinic. Int J Hyperthermia 1994;10(4):457–483.
14. Dewhirst MW, Prosnitz L, Thrall D, et al. Hyperthermic treatment of malignant disease: Current status and a view toward the future. Sem Oncol 1997;24(6):616–625.
15. Moussa N, Tell E, Cravalho E. Time progression of hemolysis or erythrocyte populations exposed to supraphysiologic temperatures. J Biomech Eng 1979;101:213–217.
16. Gaylor DC, Physical mechanism of celluar injury in electrical trauma. Massachusetts Institute of Technology. Ph. D. Dissertation 1989.
17. Doherty S, Chen B. In vivo and in vitro tissue temperature during a non-invasive 1060 nm hyperthermic fat treatment. Annual Meeting of the American Society for Laser Medicine and Surgery (ASLMS), 2016.
18. Henriques FF. Studies of thermal injury V: The predictability and the significance of thermally induced rate processes leading to irreversible epidermal injury. Arch of Pathol 1947;43:489–502.
19. Anderson RR, Farinelli W, Laubach H, Manstein D, Yaroslavsky AN, Gubeli J, Jordan K, Neil GR, Shinn M, Chandler W, Willians GP, Benson SV, Douglas DR, Dylla HF. Selective photothermolysis of lipid-rich tissue. Lasers Surg Med 2006; 38:913–919.
20. Agah R. Quantitative characterization of arterial tissue thermal damage, Master's Thesis. Austin, Texas: The University of Texas at Austin; 1988.
21. Birngruber R, Hillenkamp F. Theoretical investigations of laser thermal retinal injury. Health Physics 1985;48(6): 781–796.
22. Chen B, Thomsen SL, Thomas RJ, Oliver J, Welch AJ. Histological and modeling study of skin thermal injury to 2.0 μm laser irradiation. Lasers Surg Med 2008;40: 358–370.

APPENDIX A

The standard rate process model of tissue damage was introduced by Henriques and Moritz in the 1940's. The damage parameter Ω, which indicates the level of damage, is computed using the Arrhenius equation:

$$\Omega(r,z,t) = \ln\left\{\frac{C(0)}{C(\tau)}\right\} = A\int_0^t e^{-\frac{E_0}{RT(r,z,t')}}dt'$$

where, A is the molecular collision frequency factor, E_0 is denaturation activation energy, R is the universal gas constant, and t is the heating time. Henriques and Moritz assigned $\Omega = 0.53$ corresponding to a threshold of persistent but reversible damage, and $\Omega = 1$ to the threshold of irreversible injury. Many *in vivo* and *ex vivo* tissue studies have been conducted to derive these experimental damage constants A and E_0 for various cell/tissues (listed in Table 5). We calculated Ω based on the highest possible temperature and longest possible time of the laser treatment (25 minutes with a constant highest possible temperature 47°C). The Ω values were much smaller than 1, suggesting that: at this temperature and treatment time combination, collagen, large blood vessels, protein, and enzymes had not undergone irreversible thermal damage. In contrast, *in vitro* and *in vivo* examination of adipocyte viability by Franco et al. [5] suggested a much lower temperature threshold for adipocytes. Their data showed that adipocyte cell viability decreased to 40% at 45°C after only 3 minute exposures. Their study on *in vivo* human adipose tissue demonstrated that 15 minutes of thermal exposures to 43–45°C resulted in delayed adipocyte death. Our study also showed significant adipocyte damage can be created with a 25 minutes exposure at temperature 42–47°C.